

TABLE OF CONTENTS

	Page
Acknowledgement	iii
Abstract (Thai)	vi
Abstract (English)	ix
List of Tables	xv
List of Figures	xvi
Abbreviations and Symbols	xxiv
Chapter 1 Introduction	1
1.1. Motivation and significant	1
1.2. Objectives of the study	4
1.3. Scopes of the research	4
Chapter 2 Modeling of aortic wall	6
2.1. Circulatory system	7
2.2. Anatomy and physiology of arterial wall	10
2.3. Material model of arterial wall	11
2.3.1. Measurement of pressure and diameter of arterial	12
2.3.2. Characteristic of arterial wall	16
2.3.3. One, two and three dimension constitutive	19
equations	
2.4. Ultrasound imaging of arterial wall	22

TABLE OF CONTENTS (Continued)

	Page
2.5. Summary	24
Chapter 3 Methodology	26
3.1. Simulation of physiology modeling	28
3.1.1. Modeling the system (data analysis)	29
3.1.2. Parametric model	29
3.1.3. Model validation	31
3.1.4. Governing equation	32
3.1.5. Boundary condition setting	34
3.1.6. Equation solving	35
3.2. Mechanical modeling of blood vessel for murine aortic vessel	35
3.2.1. Experimental data harvest	36
3.2.2. Mechanical modeling	39
3.3. Mechanical modeling of blood vessel for human aortic vessel	44
3.3.1. Experimental data harvest	46
3.3.2. Mechanical modeling	49
Chapter 4 Results and discussions	69
4.1. Comparison with previous studies	70
4.2. Stresses and strains distributions of murine aortic vessel in three-dimension three-layer abdominal aortic wall based on <i>in vivo</i> ultrasound imaging	83

TABLE OF CONTENTS (Continued)

	Page
4.2.1. Parameter estimation	83
4.2.2. Boundary conditions	84
4.2.3. Principal Cauchy stresses and Green-Lagrange strains distributions across the arterial wall	87
4.3. Stresses and strains distributions of human aortic vessel in three-dimension five-layer aortic wall based on <i>in vivo</i> ultrasound imaging	90
4.3.1. Parameter estimation	90
4.3.2. Principal Cauchy stresses and Green-Lagrange strains distributions across the arterial wall	91
4.4. Effect of luminal pressure on rupture risk of aorta: case of multilayer aorta	98
Chapter 5 Limitations, suggested concepts for further research and conclusion	101
References	105
Appendix	111
Curriculum Vitae	141

LIST OF TABLES

Table	Page
2.1 Strain energy functions for study mechanical properties of arterial wall	21
3.1 Thickness of each wall layer of artery	53
3.2 Parameters A_j and B_j in unit of Pascal	60
3.3 The ultimate tensile stress and associated ultimate stretch	67
4.1 The list of number of layer, source of comparison, constitutive equation and utilized parameters for comparison our computational model	71
4.2 Two parameter sets of previous work (von Maltzahn <i>et al.</i> , 1984) and present work by using Fung's type constitutive equation for two-layer carotid artery	81
4.3 Material parameters and heart rate data of murine abdominal aortas	83
4.4 The estimated parameters	91
4.5 Levels of luminal pressure affecting arterial failure	99

LIST OF FIGURES

Figure	Page
2.1 Circulatory system (Seeley, 2003)	9
2.2 Transverse section of a large artery (Ai and Vafai, 2006)	11
2.3 Uniaxial testing of arterial strip specimen	12
2.4 Biaxial testing of arterial flat specimen	13
2.5 Formalized diagram of the apparatus. A, arterial specimen; C, collimating tube; La, light source; C.P., mercury-column manostat; Ta, tachometer; R.S-P., resolver switch-plate; R.C., resolver contacts; L, lens; P-M.T., photomultipier tube; P.M.S photomultipier power supply; M.H., manometer transducer head; M.A., manometer amplifier; X.A., X amplifier; Y.A., Y amplifier; C-R.O., cathode-ray oscilloscope. (Bergel, 1961).	14
2.6 Representative example of systolic (top) and diastolic (bottom) images of abdominal aorta recorded with intravascular ultrasound (IVUS). Boundaries of inner lumen are clearly detectable. (Hardt <i>et al.</i> , 1999)	15
2.7 Arrange of collagen fibers in the reference configuration (adapted from Holsapfel (2001)) and histological images of intimal strip, medial strip and adventitial strip with circumferential orientation (adapted from Holzapfel (2006)).	17

LIST OF FIGURES (Continued)

Figure	Page
2.8 Arterial ring in the reference configuration, in load-free configuration and in current configuration (adapted from Holzafel <i>et al.</i> (2000))	20
2.9 B-mode (Left) and M-Mode (Right) image of distal common carotid artery (Roman <i>et al.</i> , 2006)	23
3.1 Methodology for simulation of physiology modeling	30
3.2 Modeling the system	31
3.3 Mechanical Modeling	34
3.4 The system set up of mouse experiments (Danpinid, 2010)	36
3.5 A. 30 MHz ultrasound probe B. Mouse platform (left) and heart rate and temperature recorder (right) C. Experimental assembly with Vevo 770 (VisualSonics), 30 MHz ultrasound probe, mouse platform (Danpinid, 2010)	37
3.6 Experimental methodology with healthy mouse in abdomen	38
3.7 Boundary conditions	40
3.8 The pressure profile along a cardiac cycle at carotid artery of human (Male, Time step=0.140014 ms, $N=5852$ points, Cardiac cycle time=Time step*($N-1$)=0.8192 s, Heart rate=73.240 bpm). Experimental data are supported by Ultrasound and Elasticity Imaging Laboratory (UEIL), Biomedical Engineering and Radiology, Columbia University, New York, USA.	46

LIST OF FIGURES (Continued)

Figure	Page
3.9 The diameter profile along a cardiac cycle at carotid artery of human (Time step= 1/505 ms, $N = 404$ points, Cardiac cycle time= Time step*($N - 1$)= 0.7980 sec, Heart rate= 75.186 bpm). Experimental data are supported by Ultrasound and Elasticity Imaging Laboratory (UEIL), Biomedical Engineering and Radiology, Columbia University, New York, USA.	48
3.10 Schematic illustration of the geometric artery and boundary conditions	53
3.11 Mean square error and number of sinusoidal finite series relationship plotted in semi-log scale	58
4.1 Comparison result, inside radius and luminal pressure relationship by using Delfino <i>et al.</i> (1997) constitutive equation for one-layer artery (Case 1A)	72
4.2 Comparison result, inside radius and luminal pressure relationship by using Fung's type constitutive equation for one-layer artery (Case 1B)	73
4.3 Comparison result, luminal pressure and outside radius relationship by using Fung's type constitutive equation for one-layer esophageal wall (Case 1C)	74
4.4 Comparison result, outside diameter and luminal pressure relationship by using Fung's type constitutive equation for one-layer esophageal wall (Case 1D)	75

LIST OF FIGURES (Continued)

Figure	Page
4.5 Comparison of inside radius and luminal pressure relationship by using Holzapfel <i>et al.</i> (2000) constitutive equation for two-layer artery (Case 2A)	76
4.6 Comparison of principal Cauchy stresses across arterial wall at mean pressure by using Holzapfel <i>et al.</i> (2000) constitutive equation for two-layer artery (Case 2B)	77
4.7 Comparison of outside diameter and luminal pressure relationship by using Fung's type constitutive equation for two-layer carotid artery (Case 2C)	78
4.8 Comparison of luminal pressure and outside radius relationship by using Fung's type constitutive equation for two-layer esophageal wall (Case 2D)	79
4.9 Comparison of luminal pressure and outside radius relationship by using Fung's type constitutive equation for two-layer esophageal wall (Case 2E)	80
4.10 Comparison between experimental data (von Maltzahn <i>et al.</i> , 1984) and results obtained from two parameter sets of previous work (von Maltzahn <i>et al.</i> , 1984) and present work by using Fung's type constitutive equation for two-layer carotid artery	82
4.11 Contour of strain energy potential (Pa)	84

LIST OF FIGURES (Continued)

Figure	Page
4.12 Plane of longitudinal and radial directions used to show results in Figure 4.13 through Figure 4.16 for three layers of intima, media and adventitia from inside toward outside of aortic wall	85
4.13 Cauchy radial stress (kPa) distribution	86
4.14 Green radial strain distribution	87
4.15 Green circumferential strain distribution	88
4.16 Cauchy circumferential stress (kPa) distribution	89
4.17 Cauchy longitudinal stress (kPa) distribution	90
4.18 a) Plane of circumferential and radial directions used to show results in Figure 4.21 through Figure 4.22 and b) plane of longitudinal and radial directions used to show results in Figure 4.19 through Figure 4.20 for five layers of endothelium, intima, internal elastic lamina, media and adventitia from inside toward outside of aortic wall	92
4.19 Capture images of principal Cauchy stresses distributions across the $r-z$ plane deformed arterial wall in radial direction (1 st row), circumferential direction (2 nd row) and longitudinal direction (3 rd row) at DBP of 69.61 mmHg (1 st column), MBP of 89.25 mmHg (2 nd column) and SBP of 128.41 mmHg (3 rd column) obtained from the model	93

LIST OF FIGURES (Continued)

Figure	Page
<p>4.20 Capture images of principal Green-Lagrange strains distributions across the $r-z$ plane deformed arterial wall in radial direction (1st row), circumferential direction (2nd row) and longitudinal direction (3rd row) at <i>DBP</i> of 69.61 mmHg (1st column), <i>MBP</i> of 89.25 mmHg (2nd column) and <i>SBP</i> of 128.41 mmHg (3rd column) obtained from the model</p>	95
<p>4.21 Rupture area of arterial wall by using stress and strain as a criterion. (a) through (f) illustrate rupture area in plane at luminal pressure of 120, 140, 160, 180, 200 and 250 mmHg, respectively. There are five colours to identify no rupture area, i.e. violet for endothelium, light blue for intima, dark blue for internal elastic lamina (IEL), green for media and yellow for adventitia. Wherever area that ruptures, red colour is represented.</p>	96
<p>4.22 Percentage of rupture risk of arterial wall respected to physiological pressure of 100 mmHg by using stress and strain as a criterion. (a) through (f) illustrate the percentage of rupture risk in $r-\theta$ plane at luminal pressure of 120, 140, 160, 180, 200 and 250 mmHg, respectively</p>	97
<p>A.1 Thick-walled cylindrical vessel subjected to internal pressure</p>	114
<p>A.2 Components of stress relative to a cylindrical coordinate system</p>	115
<p>A.3 Triangular element showing degree of freedom</p>	116

LIST OF FIGURES (Continued)

Figure	Page
A.4 Triangular elements of abdominal aorta	116
A.5 Discretized cylinder slice	117
A.6 Effect of internal pressure on inside diameter, outside diameter and wall thickness	120
A.7 Effect of internal pressure on circumferential strain	120
A.8 Effect of internal pressure on lumen cross-sectional area	121
A.9 Effect of internal pressure on radial stress, longitudinal stress and circumferential stress	121
A.10 Circumferential stress-strain relationship	122
A.11 Radial, longitudinal and circumferential stress distributions across wall thickness at mean pressure of 96.4 mmHg of mice	122
A.12 The radial distribution of the circumferential stress $\sigma_{\theta\theta}$ in a thin walled portion of cylinder aortic vessel under an luminal pressure P_i . The circumferential stress $\sigma_{\theta\theta}$ was non-uniform but nearly constant stresses.	127
A.13 A half cut of thin cylindrical abdominal aortic vessel subjected by an luminal pressure where L , r_i and h denoted as length of vessel, inside radius and thickness, respectively.	129
A.14 Free body diagram of cylinder vessel for consideration of axial force balance	129
A.15 Components of stress relative to a cylindrical coordinate system	131

LIST OF FIGURES (Continued)

Figure	Page
<p>A.16 The B-mode image of the mouse abdominal aortic vessel (A). Pressure (mmHg) variation along a cardiac cycle (B upper) and mean diameter (mm) variation along a cardiac cycle (B lower) were shown in (B)</p>	133
<p>A.17 Relationship of current radius (mm) and Cauchy stresses (kPa) obtained from mechanical simulation analyses of thin walled (A) and thick wall (B) abdominal aortic vessel. Cauchy stresses of all three normal stresses which were radial stress, circumferential stress and axial stress was in red, green and blue line.</p>	134
<p>A.18 Relationship of radius (mm) and Cauchy stresses (kPa) obtained from mechanical simulation analysis of thick walled abdominal aortic vessel and subjected by luminal pressure of 40(A), 50(B), 60(C), 70(D), 80(E) and 90(F) mmHg.</p>	135
<p>A.19 Circumferential stress (kPa) and strain relationship</p>	136

ABBREVIATIONS AND SYMBOLS

English Alphabet

Symbol	Description
X	The position vector in reference configuration
R	Radial position in reference configuration
Z	Longitudinal position in reference configuration
x	The position vector in deformed configuration
r	Radial position in deformed configuration
z	Longitudinal position in deformed configuration
F	The deformation gradient tensor
E	The Green-Lagrange strain tensor
C	The right Cauchy Green tensor
I	Identity tensor
S	The second Piola-Kirchhoff stress tensor
G	The body force tensor of arterial wall
a	Acceleration vector
t	Time
v	Velocity vector
p	Luminal pressure
f	The body force tensor of blood
H	Thickness of arterial layer

English Alphabet

Symbol	Description
L	Overall longitudinal length in reference configuration
N	Number of experimental data points
u	Velocity component
U_{cl}	The centreline velocity
U_0	Reference bulk inflow velocity
T	Period of cardiac time
MSE	Mean square error
MBP	Mean blood pressure
SBP	Systolic blood pressure
DBP	Diastolic blood pressure
I	Principal invariant
c	Stress-like parameter of isotropic term
k_1	Stress-like parameter of anisotropic term
k_2	Dimensionless parameter of anisotropic term
A	Structure tensor of fiber direction
a_0	Fiber direction vector
b	The left Cauchy Green tensor
P	Lagrange multiplier
r_{par}	The Pearson product moment correlation coefficient from parameter estimation

English Alphabet

Symbol	Description
r_d	The Pearson product moment correlations between dependences of present study and previous studies

Greek Letters

Symbol	Description
Ω_o	The reference configuration
Θ	Angular position in reference configuration
Ω	The deformed configuration
θ	Angular position in deformed configuration
Ψ	The strain energy function
σ	The Cauchy stress tensor
ρ	Density of arterial wall
μ	Dynamic viscosity of blood
δ	Parameter for fluctuation of pulsatile flow
ζ	Fold value of mean
ξ	Fold value of amplitude
λ	Stretch ratio
Φ	Opening angle
β	Angle of collagen fibers

Subscript

Symbol	Description
<i>vol</i>	Volumetric component
<i>o</i>	Outside
<i>i</i>	Inside
<i>end</i>	Endothelium
<i>int</i>	Intima
<i>iel</i>	Internal elastic lamina
<i>med</i>	Media
<i>adv</i>	Adventitia
<i>j</i>	Arterial layer
<i>v</i>	Equivalent
<i>mean</i>	Average value

Superscript

Symbol	Description
—	Deviator component
*	Normalized value

Other symbols

Symbol	Description
∇	Gradient operator
A_0	The average height above the abscissa

Other symbols

Symbol

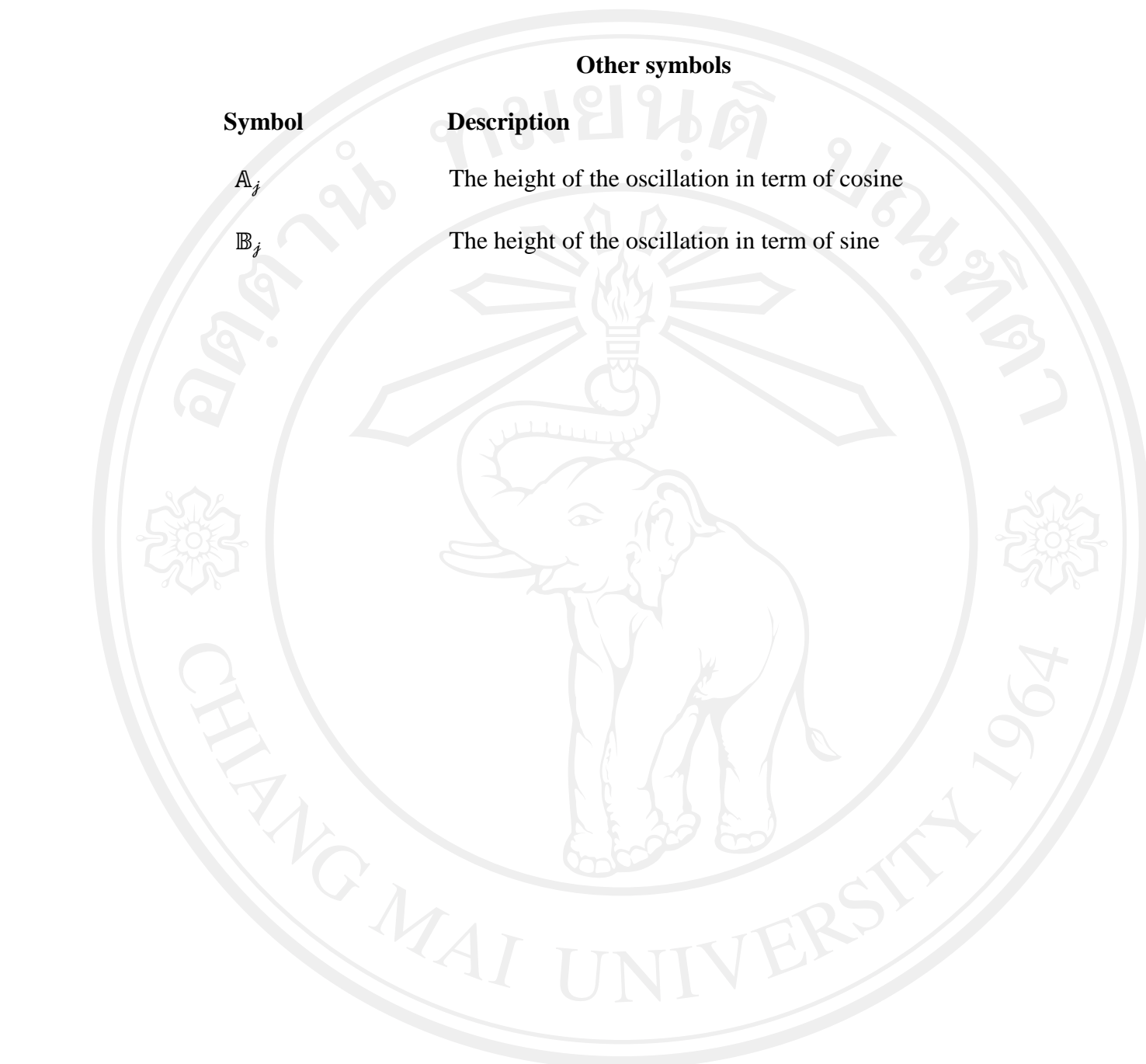
Description

A_j

The height of the oscillation in term of cosine

B_j

The height of the oscillation in term of sine



ลิขสิทธิ์มหาวิทยาลัยเชียงใหม่
Copyright © by Chiang Mai University
All rights reserved